Endoplasmic Reticulum contact sites facilitate the coordinated division of *Salmonella*-containing vacuole

Umesh Chopra[1], Priyanka Bhansali[1], Subba Rao Gangi Setty[1], Dipshikha Chakravortty[1,2*]

[1]Department of Microbiology and Cell Biology, Indian Institute of Science, Bangalore, Karnataka 560012, India

[2]School of Biology, Indian Institute of Science Education and Research Thiruvananthapuram, Maruthamala PO, Vithura, Thiruvananthapuram - 695551, Kerala, India

[*]Corresponding Author- dipa@iisc.ac.in

Abstract

Salmonella Typhimurium (STM) resides in a membrane-bound compartment called *Salmonella* containing vacuole (SCV) in several infected cell types. Within host cells, the division of bacteria and SCV are synchronous to maintain the single bacterium per vacuole. However, the mechanism regulating the synchronous fission and the machinery is not well understood. The fission of several intracellular organelles is regulated by the dynamic nature of the tubular endoplasmic reticulum (ER). In this study, we have evaluated the role of ER in controlling SCV fission. Interestingly, *Salmonella*-infected cells show the activation of unfolded protein response (UPR) with expanded ER tubules compared to the uninfected cells. Further, changing the expression of ER morphology regulators, such as reticulon-4a (Rtn4a) and CLIMP63, affected bacterial proliferation significantly, suggesting a potential role for tubular ER in facilitating the SCV division. Live-cell imaging analysis shows the marking of tubular ER precisely at the center of the majority of SCV division (78%) sites. We have investigated the role of SteA (a known *Salmonella* effector in modulating the membrane dynamics) in coordinating the SCV division. We observed that SteA

23 resides on the SCV membranes and helps in making membrane contact sites between SCV and
24 ER. Accordingly, the colocalization of ER with SCV enclosing SteA mutant *Salmonella* was
25 significantly reduced compared to SCV-formed by wild-type *Salmonella*. Depletion of *steA* in
26 *Salmonella* resulted in profound defects in SCV division, resulting in multiple bacteria residing in
27 a single vacuole with defects in proliferation compared to the wild-type strain in epithelial cells.
28 Also, during *in vivo* infection, the STM*ΔsteA* mutant shows a defect in colonization in the spleen
29 and liver and affects the initial survival rate of mice. Overall, this study suggests a coordinated
30 role of bacterial effector SteA in promoting the ER contact sites with SCVs and thus regulating the
31 successful division of SCV.
32

Introduction

Salmonella enterica subsp. *enterica* serovar Typhimurium (STM) is an intracellular pathogen known to infect a wide range of hosts and result in diseases across species, including gastroenteritis to systemic infections [1], [2]. *S.* Typhimurium enters the body through the fecal-oral route following the bacteria utilize an arsenal of strategies to overcome several stresses like the acidic pH of the stomach, gut flora, bile salts, etc., and finally reach the small intestinal epithelia [3]. *Salmonella* secretes several virulence proteins inside the cell, which leads to actin rearrangement and membrane ruffling, which helps in the invasion of bacteria inside the host epithelial cell [4], [5], [6], [7]. *Salmonella* effector SopD is known to facilitate the recruitment of dynamin2 (Dyn2) at the invasion site, which helps in the endocytosis of bacteria inside host cells [8].

Upon invasion into the host cell, *Salmonella* resides in *Salmonella* containing vacuole (SCV), a membrane-enclosed compartment. Mature SCV shares several characteristic markers with lysosomes/late endosomes such as LAMP1 and Rab7 but is negative for acid hydrolases and cathepsins [9]. Inside the epithelial cells, several protruding structures from SCV known as *Salmonella*-induced filaments (SIFs) are observed, which are LAMP1 positive [10], [11]. The membrane composition of SCV is not very well understood, but it contains molecules and proteins from several host organelles and is enriched with several bacterial effector proteins [12], [13]. Our group, as well as several others, have previously shown that *Salmonella* resides as a single bacterium per vacuole state inside the host, suggesting that SCV membrane divides synchronously with the division of *Salmonella* but the mechanism behind SCV division is not known [14], [15], [16], [17]. For successful SCV division, expansion of SCV membrane, pinching of SCV membrane

precisely with bacterial division, and lastly, scission of host-derived SCV membrane must be followed in an orchestrated manner.

Several literatures have highlighted the importance of contact sites between cellular organelles, such as contact sites of ER with mitochondria, plasma membrane and endosomes, and contact sites between mitochondria with lysosomes [18], [19], [20], [21]. Contact sites between ER-mitochondria and ER endosomes are very widely studied in the aspect of organelle division [18], [22]. In the case of mitochondria, which comprises an inner and an outer membrane, both membranes divide simultaneously during its fission. The inner mitochondrial membrane uses its machinery for fission, while outer membrane constriction is initiated by the ER, followed by the recruitment of Drp1, which mediates the fission of mitochondria [18], [23], [24]. Bacterial pathogens like *Chlamydia* and *Brucella* make contact sites with cellular organelles to facilitate their proliferation inside the host cell [25], [26], [27]. Interestingly, the SCV membrane also comprises several ER proteins, and recently, membrane contact sites between SCV and ER have also been observed [28]. To understand the mechanism behind the SCV division, we reasoned that SCV is partially like mitochondria. SCV and mitochondria (being an endosymbiont) encompass an outer membrane derived from the eukaryotic host, while the inner membrane of mitochondria is prokaryotic in nature, like the cell wall of *Salmonella*. To understand the same, we hypothesized that a process similar to mitochondria could lead to SCV division. Our results suggest that *Salmonella* infection leads to activation of UPR, ER expansion, and an increase in ER tubulation. We have observed ER tubules mark at the fission site of SCV division which possibly initiate the constriction. *Salmonella* translocated effector SteA localizes onto the SCV membrane and possibly helps in making contact with ER, suggesting that SteA can act as a factor to recruit the ER onto SCV and thus facilitate the SCV division. STM*ΔsteA* resides as multiple bacteria in one big

77 vacuole with defects in proliferation. During *in vivo* infection, STM*ΔsteA* shows defects in
78 colonization in the spleen and liver if injected through the intraperitoneal route. Also, there is a
79 delay in the onset of mice death upon infection with STM*ΔsteA* as compared to STM WT, but
80 eventually, mice succumbed to death on the 8th day post-infection. Overall, our study unravels,
81 for the first time, the coordinated role of ER and bacterial effector SteA in successful SCV division
82 inside the cell.

83

84

85 **Materials and Methods**

86 **Bacterial strains and culture conditions**

87 *Salmonella enterica* subspecies *enterica* serovar Typhimurium (STM WT) wild-type strain ATCC
88 14028s was used in all experiments. The bacterial strain was cultured in Luria broth (LB-Himedia)
89 with constant shaking (170 rpm) at 37°C orbital-shaker. Antibiotics like kanamycin (50 µg/ml) and
90 ampicillin (50µg/ml) were used wherever required. A one-step gene inactivation method was used
91 for the generation of knockout strains [29]. Wild type as well mutant strains were transformed with
92 pFPV-m-cherry or pFPV-GFP plasmid for immunofluorescence assays.

93 Table:1 List of bacterial strains used in this study

Strain	Characteristic (Antibiotic resistance)	Source
STM WT 14028s	-	Kind gift by Prof. M. Hensel
STM*ΔssaV*	Kan^R	Laboratory stock
STM*ΔsteA*	Kan^R	This study
STM*ΔsteA:steA*	Kan^R +Amp^R	This study

94

95 **Generation of Complement strain and SteA-eGFP plasmid**

96 Low copy number plasmid pQE-60 was used to prepare the SteA-HA complement strain. Briefly,
97 PCR amplification (using Thermo Q5 DNA polymerase) of the *steA* gene was performed using
98 Wild Type STM colony with respective PCR primers. Forward cloning primer was chosen from a
99 position of 250 base pairs upstream of the gene start site to amplify the native promoter of the gene
100 during PCR and to maintain the native expression level of protein, and the sequence of HA tag was
101 added in reverse primer. The amplified PCR product was purified using a Gel extraction kit
102 (Qiagen). The PCR product and Plasmid were subjected to restriction digestion by using Xho1
103 (NEB) and Hind III (NEB) at 37°C for 2 hours. The double-digested PCR product and plasmid
104 were further subjected to Ligation using T4 DNA ligase (NEB) at 16°C for 12-14 hours. The
105 ligated product was further electroporated in STMΔ*steA* strain to prepare the complemented strain,
106 i.e., STM*ΔsteA*:pQE60-*steA* (hence referred to as STM*ΔsteA:steA*). The expression level of
107 complement was confirmed with western blotting and confirmed with DNA sequencing.

108 For preparation of SteA-eGFP plasmid for transfection study, eGFP-N3 empty vector was used.
109 The sequence of *steA* was amplified via PCR from STM WT using primer with restriction site for
110 Xho1 and BamH1. The entire process for cloning was performed as discussed above.

111 **Eukaryotic Cell Culture, Transfection and Plasmids**

112 HeLa cells and RAW 264.7 murine macrophages were cultured in DMEM (Lonza) containing 10%
113 FBS (Gibco) at a humified incubator, maintaining a temperature of 37°C and 5% CO_2. Cells were

114 seeded in 6 wells, 12 wells, or 24 well plates at a confluency of 60-70% prior to infection. Cells
115 were maintained in the presence of 1% penicillin and streptomycin (penstrep). Cells were given a
116 PBS wash and supplemented with fresh media without penstrep at least 6 hours prior to infection.
117 Plasmid overexpression or knockdown via shRNA was done using Lipofectamine 3000 using
118 manufacturer protocol. Briefly, 300ng of plasmid was mixed in opti-MEM media for 5 min while
119 1ul of L3000 was added (for one well of 24 well plates) in opti-MEM for 5 min separately and
120 further mixed and incubated for 20 min at room temperature. Post incubation, this mixture was
121 added to cells for 6 hours for transfection to take place. Cells were washed with PBS and
122 supplemented with complete media post 6 hours of treatment, and post 48h of transfection,
123 infection was given. Overexpression constructs such as pHAGE2 mCherry-Rtn4a was a kind gift
124 from Prof. Tom Rapoport (Addgene plasmid 86683) [30] mCh Climp-63 and mCh sec61β was a
125 kind gift from Prof. Gia Voeltz (Addgene plasmid 136293, Addgene 49155) [31], [32], RFP KDEL
126 construct was a kind gift from Prof. Nagaraj Balasubramanian [33], GFP-LAMP1 was provided
127 by Prof. Mahak Sharma [34]. The shRNA plasmids were obtained from the human genome-wide
128 TRC shRNA library (purchased from Sigma-Aldrich, USA, Catalog no. SH0411), available at
129 shRNA resource centre, MCB, IISc. pLKO.1-puro non-mammalian shRNA (SHC002, shControl)
130 was used as a control in all the shRNA mediated knockdown experiments. Plasmid sequences and
131 details are added in supplementary table 2.

132 **Protocol for infection (Gentamicin Protection Assay)**

133 The cells were seeded at the required confluency and infected with *Salmonella* strains with actively
134 growing log phase culture (for epithelial cells) and stationary phase culture (for RAW 264.7
135 macrophages) at Multiplicity of infection (MOI) 10 for Intra Cellular Survival Assay (ICSA) and

136 confocal imaging. For the live cell imaging experiment, an MOI of 25 was used to increase the
137 event of finding infected cells for imaging. For confocal microscopy studies, cells were seeded on
138 sterile glass coverslips at least 24 hours before infection. Upon infecting the cells at the required
139 MOI, the plate was centrifuged at 600 rpm for 5 min to facilitate the adhesion, and then the plate
140 was incubated for 25 min at 37°C and 5% CO_2. Post incubation, bacteria-containing media was
141 removed, and cells were given 2 PBS washes to remove any extracellular bacteria. Fresh media
142 containing 100µg/ml of gentamicin was added into wells and incubated at 37°C for one hour.
143 Following this, cells were again given 2 PBS washes, and fresh media containing 25µg/ml of
144 gentamicin was added, and this concentration was maintained till the end point of the experiment.
145 Cells were harvested at required time points, such as 2h and 16h for ICSA, 2h, 6h, and 16h for
146 confocal microscopy-based experiments.

147 **Confocal Microscopy**

148 After an appropriate hour post-infection, cells were washed with PBS twice and fixed with 3.5%
149 PFA at room temperature for 15 min. After fixation, coverslips were washed with PBS, and cells
150 were stained with primary antibody prepared in 2% BSA in PBS carrying 0.01% of saponin (for
151 membrane permeabilization) for 1 hour at room temperature or 4°C overnight in a cold room as
152 required. Post incubation, coverslips were washed again twice with PBS and incubated with
153 specific secondary fluorophore-labeled antibodies and incubated for one hour at room temperature.
154 Coverslips were then mounted on clean glass coverslips using mounting media. Once the mounting
155 media was dried, coverslips were stabilized by sealing the periphery with transparent nail paint on
156 the sides. Images were acquired on a confocal scanning laser microscope (Zeiss 880 multiphoton
157 microscope or Leica sp8 falcon system with or without zoom as required). Zen black software was
158 used for all colocalization-based quantification and to calculate mean fluorescence intensity (MFI).

159 Calculations of CTCF, percent of ER tubules, SCV diameter, and Line scans were prepared using
160 ImageJ. The ER tubule percentage is calculated by calculating the sheet percentage from the total
161 cell area. Sheet area / total area *100 = Sheet area percentage and further 100 - Sheet area
162 percentage = tubule area percentage [35]. Live cell microscopy was performed on the Leica SP8
163 Falcon microscope, and live cell video was processed and prepared using LAS X software.
164 Antibodies used in this study are mentioned in supplementary table 3.

165 **Bacterial enumeration after infection for Intracellular survival assay**

166 After the appropriate hour of post-infection, cells were washed with PBS at RT and lysed using
167 0.1% Triton-X 100. Cell lysate was plated on SS agar to obtain colony forming unit (CFU) and it
168 was used for the calculation of Percent Invasion and Fold proliferation using this formula.

169 Percent Invasion: (CFU obtained at 2 hours post-infection/ CFU obtained from pre-inoculum)
170 *100

171 Fold proliferation: CFU obtained at 16-hour post-infection/CFU obtained at 2 hours PI

172 **RNA isolation and Real-Time PCR (qRT-PCR)**

173 RNA isolation was performed using TRIzol (Takara) following the manufacturer's protocol.
174 Quantification of RNA was done using nano-drop (Thermo-Fisher Scientific) and RNA samples
175 were run on 1% agarose gel to check the quality of RNA. 2 µg of RNA was subjected to DNase I
176 (Thermo Fischer Scientific) treatment at 37°C for 1 hour followed by addition of 0.5M EDTA
177 (final concentration 5mM) and heat inactivation at 65°C for 10 mins to inactivate the enzyme.
178 Further, cDNA was prepared by using a cDNA synthesis kit (Takara) as per the manufacturer's
179 instructions. The expression profile of all genes of interest was evaluated using RT primers by
180 using SYBR green mix (Takara) in a Biorad Real-Time PCR machine. The expression value of

181 the target gene was normalized to housekeeping internal control β-actin and further compared with
182 uninfected cells. Primers used in this study are mentioned in Supplementary Table 4.

183 ***In vivo* animal experiment**

184 6-8 weeks old C57BL/6 female mice were infected by orally gavaging 10^7 CFU of STM WT,
185 STM*ΔsteA* and STM*ΔsteA:steA*. 5 days post-infection, mice were euthanized, and organs such as
186 liver, spleen, MLN, and blood were harvested to study the colonization in organs. For
187 intraperitoneal injection, 10^3 CFU of bacteria was administered per animal, and 3 days post-
188 infection, organs were homogenized and further plated on *Salmonella-Shigella* agar. Obtained
189 CFU values were normalized with the gram weight of the organ and then converted into a log
190 scale. Blood was collected through heart puncture and plated on SS agar. For the mice survival
191 assay, 10^8 CFU was administered to each mouse via oral gavage. Mice were monitored every
192 day till the time none of the mice in the cohort survived. The animal experiments were carried
193 out in accordance with the approved guidelines of the institutional animal ethics committee at the
194 Indian Institute of Science, Bangalore, India (Registration No: 48/1999/CPCSEA). All
195 procedures involving the use of animals were performed according to the Institutional Animal
196 Ethics Committee (IAEC)-approved protocol.

197

198 **Statistical analysis:**

199 Statistical analysis was performed using GraphPad Prism software. For analysis, the student's t-
200 test (unpaired parametric test) was performed. The results are indicative of mean± SD or mean±
201 SEM. To calculate the statistical significance of bacterial colonization *in vivo*, the Mann-
202 Whitney test was performed. Group size, experimental number, no of cells in each set, and P
203 value of each experiment are described in figure legends.

204

205 **Results**

206 ***Salmonella* infection leads to the activation of UPR and expansion of the Endoplasmic**
207 **Reticulum**

208 Several bacterial and viral infections are known to activate UPR for their survival [36], [37]. UPR
209 helps to alleviate the ER stress by initiating several transcriptional and translational regulations
210 which lead to the maintenance of ER homeostasis [38], [39]. Inside the cell, UPR signaling is
211 maintained by transmembrane proteins located in the ER membrane and their catalytic domain
212 towards the cytosol. Inositol requiring enzyme-1 (IRE-1), Protein kinase c like ER kinase (PERK),
213 and Activating transcription factor-6 (ATF-6) comprises the main arm of UPR. Recent reports have
214 shown the contact of SCV with ER, also the presence of ER proteins in the membrane fraction of
215 SCV suggests the crosstalk between them [12], [28]. Here, we investigated how *Salmonella*
216 infection modulates the ER dynamics. To understand the activation of UPR by any of these
217 pathways, we used confocal microscopy and quantified the translocation of downstream
218 transcription factors, such as XBP1, ATF4, and ATF6, inside the nucleus upon infection. SPI2
219 mutants of *Salmonella*, STM*ΔssaV* (which is unable to secret SPI-2 encoded effector protein in
220 host cytosol) was kept as a control to understand if activation of UPR is mediated by bacterial
221 effectors or dependent on bacterial invasion. Our results suggest that from as early as post 2h of
222 *Salmonella* infection, both the transcription factors, ATF4 and ATF6 from the cytosol translocated
223 to the nucleus of infected cells as compared to uninfected cells and STM*ΔssaV* infected cells,
224 suggesting that only wild-type *Salmonella* can activate UPR (fig 1A-1D). *Salmonella*-induced
225 ATF4 and ATF6 translocation were retained till 16h post-infection (fig S1A-S1D). However, we

226 didn't observe any increase in XBP1 recruitment inside the nucleus (fig 1E,1F) upon infection at
227 any time point post-infection (fig S1E, S1F), suggesting that *Salmonella* infection upregulates
228 UPR by PERK and ATF6 pathways in HeLa cells. To alleviate the ER stress, activation of UPR
229 leads to the expansion of the ER, protein folding capacity, and increased phospholipid production
230 [40]. Increased bacterial proliferation requires a continuous source of membrane for the increasing
231 number of SCV, and increased phospholipid production upon UPR could facilitate the SCV
232 proliferation inside the host cell. Therefore, we sought to determine if *Salmonella* infection led to
233 ER expansion during the pathogenesis phase. Our transcriptional analysis suggests that upon
234 infection, there is upregulation at the transcript level of ER shaping proteins such as *Climp63*
235 (responsible for maintaining ER sheets) and *Reticulon-4a* (*Rtn4a*, essential for maintaining ER
236 tubules) (fig 1G, fig 1H). The upregulation was significantly observed at the late time point of
237 infection, i.e., 16h post-infection, suggesting that active proliferation of *Salmonella* and not just
238 invasion (as evident at 2h and 6h post-infection) leads to ER expansion.

239 Since an increase in the transcript levels of ER shaping proteins was observed at the later time of
240 infection, we tried to quantify the percentage of ER sheets and tubules using the ER marker, RFP-
241 KDEL, upon infection to understand ER expansion. Upon analysis of microscopy images, we
242 observed that *Salmonella*-infected cells showed an increased percentage of ER tubules compared
243 to uninfected cells (fig1I, fig1J). The changes in percent ER tubules were only evident in infected
244 cells as compared to uninfected and bystander cells (neighboring cells that are not infected),
245 suggesting that stabilized SCV and bacterial effectors are responsible for this phenotype (fig S1G
246 and S1H). Together, this data indicates that *Salmonella* infection leads to changes in ER
247 morphology.

248

249 **Expansion of ER tubules facilitate SCV proliferation and its division**

250 Dynamic ER tubules play an essential role in forming membrane contact sites with several
251 organelles [41], [42]. Figure 1 indicates that actively proliferating bacteria increased tubular ER
252 and upregulated the expression of *Rtn4a*. We also tried to understand if there is an advantage of
253 the increased tubules to bacterial proliferation. To identify the role of ER tubules in mediating
254 bacterial proliferation, we transiently overexpressed reticulon 4a (Rtn4a) in HeLa cells, which
255 helps to increase ER tubules [43], and then quantified the proliferation of bacteria by intracellular
256 survival assay (ICSA). As compared to empty vector and general ER marker sec61β-mCh control,
257 increased ER tubulation by Rtn4a led to the higher proliferation of *Salmonella* with no significant
258 change in percent invasion, suggesting an increase in ER tubules helps in bacterial proliferation
259 (fig2A, figS2A). To validate if this change in proliferation was dependent solely on the function
260 of Rtn4a, knockdown of Rtn4a via shRNA was performed (figS2B). Knockdown of Rtn4a (˜40%
261 reduction at transcript level) led to reduced proliferation of bacteria as compared to scrambled
262 control, hence strengthening the crucial role of ER tubules in bacterial proliferation (fig2B).
263 Climp63 overexpression led to an increase in ER sheets as opposed to tubules. We quantified the
264 number of SCV per cell upon transiently overexpressing the Climp63 in HeLa cells. Our data
265 indicated that the number of SCV present per cell decreases upon overexpressing ER sheets using
266 Climp63 compared to controls (fig2C, fig2D). Division of *Salmonella* is linked with the fission of
267 SCV membrane [15]. Since the intricate balance of ER sheets and tubules affects bacterial
268 proliferation, we hypothesized that ER tubules might facilitate SCV fission. In the case of
269 mitochondria, membrane-less organelle, and endosomes, ER marks the division site, and later

270 fission is completed by Drp1 (in mitochondria) and coronin1c and TMCC 1 complex (in
271 endosome) [18], [24], [44], [45]. To investigate our hypothesis of ER tubules playing a role in SCV
272 fission, we performed live cell imaging in cells transfected by RFP-KDEL (to mark the ER)
273 followed by infection with *Salmonella*. Quantification of data suggests that ER tubules mark the
274 division site precisely at the center of dividing SCV in 78% of events, as observed by image
275 snapshots and corresponding line scans (fig2E-G, video S1). STM WT infected RAW macrophage
276 also showed contact of ER on the dividing bacteria (video S2, S2C). This was also evident in fixed
277 cell images where we could observe Lamp1 enclosed *Salmonella* division in SCV marked by ER
278 tubules exactly in the center in 56.7±6.61% of fission events, however, in 14±9.07% of events, ER
279 was seen in proximity to the center and hence mentioned as adjacent while 29.2±8.4% of dividing
280 SCV did not possess ER tubules on them (fig2H, fig2I). This data suggests the importance of ER
281 tubules in marking the fission site of SCV. Taken together this data suggests that ER tubules help
282 in the proliferation and division of SCV by marking the fission site inside the cell and help in
283 maintaining SCV number within the cell.

284 ***Salmonella* translocated effector SteA is crucial for maintaining SCV contact site with ER,**
285 **resulting in a single bacterium per vacuole**

286 SCV division leads to a single bacterium per vacuole throughout the course of pathogenesis in cell
287 lines or *in vivo* [14]. Domingues et al., suggested the role of SteA in maintaining the membrane
288 dynamics of SCV [46]. In accordance with the same, we also observed that *steA* mutant strain of
289 *Salmonella* (STM*ΔsteA*) resides as multiple bacteria in one single vacuole (fig 3A). Our data
290 suggests that compared to STM WT, 30±3% of mutant bacteria reside in one big vacuole,
291 suggesting that loss of function of *steA* leads to improper SCV fission (fig 3B). Live cell imaging

292 shows several points of contact between SCV and ER, suggesting that SCV actively makes
293 membrane contact sites with ER for its survival and proliferation (fig 2E, fig 3C). SteA resides
294 onto the PI4P-enriched SCV membrane (fig 3C), and hence, we asked if membrane contacts
295 between ER and SCV are maintained by SteA. Microscopy images show that SteA-enriched SCV
296 makes contact with ER (fig 3C). Quantification of the data suggests that ER colocalizes more with
297 the SCV of STM WT than the SCV formed by STM*ΔsteA* (as observed colocalization between
298 SCV marker Lamp1 and RFP KDEL), suggesting that SteA helps in making contact sites of SCV
299 with ER (fig 3D, fig 3E). This was also observed upon transfecting HeLa cells with the SteA-eGFP
300 construct, where SteA-eGFP showed higher colocalization with ER marker RFP-KDEL as
301 compared to eGFP empty vector control, strengthening the fact that SteA possibly associate with
302 ER (figS3A, S3B). Overall, this data suggests that SteA might help in making contact sites with
303 ER and further recruiting ER onto the SCV. These contact sites can be used as a stealthy approach
304 by *Salmonella* to recruit membrane from ER, and along with other *Salmonella* effector proteins,
305 facilitating SCV fission.

306 **STM*ΔsteA* shows a defect in proliferation and pathogenicity *in vivo***

307 Previous reports from our lab suggested that *Salmonella* utilizes the strategy of SCV division to
308 increase the number of SCV per cell, so it becomes difficult for the cellular system to eradicate the
309 growing SCV [14]. Since *steA* mutants form a big vacuole inside the cell, we asked how the mutant
310 strain proliferates in the cell. As compared to STM WT and STM*ΔsteA:steA* (complemented
311 strain), STM*ΔsteA* proliferated significantly less in the HeLa cell line. (fig4A). Less proliferation
312 of mutant strain suggests that those bulky vacuoles might be targeted by cellular machinery for
313 degradation. Quantification of vacuole size suggests that the diameter of SCV formed by

314 STM*ΔsteA* is around 6.9±3.13µm whereas SCV of STM WT is 0.4±0.11µm (fig4B, fig4C). Using
315 LC3B as a marker to detect the extent of autophagy, we observed that LC3B colocalized more with
316 SCV of *steA* mutants as compared to SCV of STM WT at 16h post-infection (fig4D, fig4E).
317 Actively proliferating *Salmonella* also reduces the number of lysosomes inside the cell to escape
318 its fusion with acidic lysosomes [14]. In STM*ΔsteA* infected cells, we observed a higher intensity
319 of Lamp1 similar to uninfected cells, suggesting that STM*ΔsteA* is unable to change the lysosomal
320 dynamics as opposed to STM WT. A higher flux of lysosomal proteins, along with the recruitment
321 of LC3B, led to less proliferation of the STM*ΔsteA* inside the cell (figS4A, figS4B). Next, we were
322 interested in understanding the pathogenicity of STM*ΔsteA in vivo*. For this, we intraperitoneally
323 injected 10^3 CFU of *Salmonella* per C57BL/6 mice, and 3rd-day post-infection mice were
324 euthanized, and organs such as liver and spleen were harvested to observe organ burden. Our data
325 suggest that 3rd-day post-infection, STM*ΔsteA* shows less colonization in the spleen and liver as
326 compared to STM WT and STM*ΔsteA:steA* (fig 4G, fig4H). To further understand the
327 pathogenicity of the mutant strain, we orally gavaged C57BL/6 mice with 10^7 CFU of STM WT,
328 STM*ΔsteA*, and STM*ΔsteA:steA,* and 5 days post-infection, mice were euthanized, and organs such
329 as liver, spleen, and mesenteric lymph nodes were harvested since they act as a secondary site of
330 infection (fig4J-4L). We observed no significant change in the colonization of bacteria in these
331 organs, suggesting STM*ΔsteA* doesn't lose its capability to cross the gut barrier and colonize and
332 disseminate in distal organs and blood if injected through the oral route (figS4C). However, upon
333 performing a survival assay of mice upon infection through oral gavage, we noticed the delayed
334 onset of mice death in the STM*ΔsteA* infected cohort (fig4M), where STM WT infected mice
335 started succumbing to infection from 5th day post-infection, STM*ΔsteA* infected cohort started
336 succumbing to infection at 7th day post-infection, and at 8th-day post-infection, all the mice

337 succumbed to death. Taken together, this data suggests that if the fission of SCV is altered,
338 *Salmonella* resides as multiple bacteria in one big vacuole and proliferates less. Those big/bulky
339 vacuoles are further targeted by autophagic machinery and cleared by active lysosomes in the cell
340 culture system. During *in vivo* infection through the intraperitoneal route, STM*ΔsteA* shows
341 defects in colonization in the spleen and liver and also affects the initial survival rate of mice,
342 suggesting that SteA acts as an essential effector for pathogenicity in mice.

343

344 **Discussion:**

345 Bacterial pathogens invade several cell types and reside in endocytic or phagocytic vacuoles [47].
346 Cell uses their extraordinary machinery to clear the pathogens, but by using several effector
347 proteins, bacterial pathogens modulate cellular machinery and prolong their survival. A few
348 strategies that several bacterial pathogens utilize are: modification of the membrane of the
349 pathogen-containing vacuole, blocking the activation of xenophagy, and escaping its fusion with
350 acidic lysosome [48], [49], [50], [51], [52], [53], [54]. Bacterial pathogens such as *Legionella,*
351 *Brucella, Chlamydia*, and *Salmonella* are known to reside in vacuoles, but the morphology and
352 membrane source of the vacuole are quite different. *Legionella* and *Chlamydia* reside in a spacious
353 vacuole that comprises multiple bacteria in a single vacuole [55], contrary *Salmonella* resides in a
354 tight-fitting vacuole as a single bacterium per vacuole [14]. The biogenesis of the SCV membrane
355 is not very well known, but proteome analysis of SCV suggests that the SCV membrane is highly
356 modified and contains proteins from the lysosome, Golgi, and ER [12]. Several effectors of
357 *Salmonella* help in recruiting membrane components, inhibiting the transport of M6PR, and
358 making contact sites with organelles for its proliferation [56], [57], [58]. Our results suggest that

359 *Salmonella* infection induces ER stress inside the cell and activates the UPR. A few ways by which
360 UPR helps in alleviating stress are 1) by increasing the protein folding capacity of cells and 2) by
361 expanding the ER. Our data suggests that wild-type STM infection leads to UPR activation while
362 STM*ΔssaV* is unable to activate the UPR arm. This suggests that bacterial effectors are crucial for
363 initiating ER stress, as it was evident as early as 2h post-infection. Our studies support the previous
364 findings, which suggest *Salmonella*-induced ER stress is crucial for bacterial proliferation [59],
365 [60], [61]. Further, UPR activation leads to an increase in phospholipid production [40], which
366 could be useful for the bacteria as growing SCV requires a continuous source of membrane.
367 *Salmonella*-infected cells show an increase in expression of *Reticulon-4a* and *Climp63* with an
368 increase in tubular ER, suggesting this is an active strategy employed by bacteria for its survival.
369 Exogenously overexpression of Rtn4a provides an advantage in the proliferation of *Salmonella*;
370 however, reduction in ER tubules by knockdown of Rtn4a or overexpression of ER sheets using
371 Climp63 negatively affects the bacterial proliferation and SCV number inside the cell, indicating
372 ER tubules plays a crucial role in bacterial proliferation. The intricate balance of ER sheets and
373 tubules has been recently shown to affect the dynamics of membrane-less organelle [42]. Our study
374 also highlights the importance of ER in the successful proliferation of *Salmonella*. Our live cell
375 data showed the recruitment of ER tubules at the center of dividing SCV. This was evident in HeLa
376 as well as RAW 264.7 macrophage cell lines, suggesting that ER tubule recruitment marks the
377 division site of SCV and leads to a single bacterium per vacuole. ER is very well known for
378 marking the division site of organelles such as mitochondria, membrane-less organelle, and
379 endosomes [18], [42]. Our study suggests that *Salmonella* hijacks the strategy of ER recruitment
380 for its survival and SCV division. We have identified the role of bacterial effector SteA in
381 maintaining the contact of SCV with ER in the formation of possible membrane contact sites.

382 Earlier studies have shown the presence of SteA on SCV and its colocalization with Golgi [62],
383 [63], [64]. In our study, we have partially observed a similar phenotype and have observed a new
384 role of SteA in interaction with ER. Inside the infected cell, the expression of SteA is highly
385 regulated as it can be mostly seen around the bacteria onto SCV. To investigate the role of SteA in
386 making contact sites, we looked for the colocalization of ER with SCV of STM WT and
387 STM*ΔsteA*. We observed the difference in colocalization of ER with SCV, highlighting the
388 importance of *the Salmonella* effector SteA in mediating the contact site between SCV and ER.
389 Bacterial pathogens such as *Chlamydia* use its effector protein for forming contacts of its inclusion
390 bodies with ER [25] and it also targets host cellular protein to facilitate this interaction [65].
391 *Salmonella* effectors SseJ and SseL have previously been reported to recruit OSBP1 onto SCV,
392 which helps in making contact with VapA and VapB (conserved ER proteins known for tethering
393 of ER with cellular organelles) and maintain SCV vacuolar integrity [66]. Our data suggests the
394 potential role of SteA in forming contact sites of SCV with ER as a strategy to facilitate its
395 proliferation.

396 The loss of function of SteA led to a bulky vacuole carrying multiple bacteria inside and with
397 defects in proliferation. Evidence from McQuate *et al*., also suggests the defect in the proliferation
398 of STM*ΔsteA* in epithelial cells as well as macrophages [62]. To understand the difference in
399 proliferation of STM*ΔsteA* compared to STM WT, we have observed SCV formed by STM*ΔsteA*
400 colocalizes more with autophagy marker LC3B, suggesting big bulky vacuoles are cleared by the
401 cellular system and hence lead to less proliferation inside the cell. STM WT also actively reduces
402 lysosome number inside the cell as an active strategy to block its fusion with the acidic lysosome
403 [14]. But in the case of STM*ΔsteA* infected cell, we observed a higher mean intensity of LAMP1,
404 which was similar to the intensity observed in uninfected cells, suggesting that somehow

405 STM*ΔsteA* could not modulate lysosomal dynamics and, as a result, active lysosome could hinder
406 the bacterial proliferation in cell line model. Similarly, Liu *et al*.,2021 have highlighted the
407 importance of SteA in bacterial proliferation inside cells by impairing the fusion of SCV with
408 lysosomes [67]. Taken together, this data suggests the importance of SteA in bacterial proliferation
409 inside infected cells. STM*ΔsteA* also showed defects in colonization in the spleen and liver if
410 infected through the intraperitoneal route, suggesting SteA is crucial for *in vivo* pathogenicity.
411 However, to our surprise, we did not observe any defect in the *in vivo* colonization of mouse organs
412 such as the liver, spleen, MLN, and blood if infected through the oral gavage route. Survival
413 analysis of mice suggests late onset of mice death in STM*ΔsteA* infected cohort upon infection as
414 compared to STM WT. We have also observed less weight reduction in STM*ΔsteA* infected mice
415 cohort as compared to STM WT, and this difference in weight reduction could provide an
416 advantage in the initial survival rate of STM*ΔsteA* infected mice. (figS4D). Alongside, Geddes *et*
417 *al*., 2005 have reported the importance of SteA for efficient colonization in mouse spleen using the
418 Balb/c mice model infecting via the intraperitoneal route [63]. We have also observed similar
419 defects in the spleen using C57BL/6 mice. However, upon infection through oral gavage, there are
420 no defects in the colonization of STM*ΔsteA* in organs. This observation suggests that the route of
421 infection can severely affect bacterial colonization and pathogenicity. Infection through the
422 intraperitoneal route bypasses the gut-intestinal barrier, while during oral gavage, *Salmonella* faces
423 several challenges, from the acidic pH of the stomach to several metabolites in the intestinal lumen.
424 More studies are needed to understand this difference in colonization rate depending on the route
425 of infection. Alongside, further investigations are needed to understand the vacuolar status of SCV
426 during *in vivo* infection if infected through oral or intraperitoneal route to understand the difference

427 in pathogenicity. Taken together, our study suggests the importance of SteA in bacterial
428 pathogenicity and proliferation.

429 Our study provides new insights into how bacteria use a strategy of remodeling the ER dynamics
430 for its benefit. Domingues et al.,2014 and Chen et al.,2021 have highlighted the importance of
431 SteA for the active division of SCV [46], [68]. Our data supports their findings and suggests the
432 possible role of SteA in recruiting the ER and facilitating SCV fission. Interestingly, where wild-
433 type STM can easily divide along with SCV, while loss of function of SteA hampers 30% SCV
434 division with marked less colocalization with ER, suggesting there can be several other effector
435 proteins that might facilitate the contacts between ER and SCV. As reported by Chen et al.,2021
436 about the coordinated role of SteA, SopD2, and SifA in successful SCV division, our data explains
437 the newly identified role of SteA in the process by making contact sites with ER. Since these
438 effectors have coordinated roles, it will be interesting to understand how individual bacterial
439 effectors are crucial in the complete fission of SCV. Several host proteins have also been linked
440 with SCV division as the absence of those host proteins, such as PLEKHM1 and ESCRT-3, leads
441 to SCV carrying multiple bacteria [57], [69]. Within the cell, SCV acts as an autonomous organelle
442 that has acquired a vacuolar membrane from the host system, which also synchronously divides
443 along with bacterial division. The machinery regulating the SCV division could be difficult to
444 identify because these fission events are very transient in nature. As per literature evidence, both
445 host and bacterial effectors could be equally involved in this process to execute successful fission.
446 A complete knowledge of fission machinery can be used as a targeted approach to inhibit bacterial
447 proliferation during infection.

448 **Acknowledgements**

We acknowledge the Departmental and Divisional Confocal Microscopy Facility and Central Animal Facility at IISc for providing us with an opportunity for experimentation. Mr. Sumitlal K and Ms. Navya have helped in image acquisition in Confocal Microscopy.

Funding information

We express our heartfelt gratitude to the financial support from the Department of Biotechnology (DBT), Ministry of Science and Technology; Department of Science and Technology (DST), Ministry of Science and Technology. DC acknowledges DAE for the SRC Outstanding Investigator Award and funds, ASTRA Chair Professorship, and TATA Innovation fellowship funds. The authors jointly acknowledge the DBT-IISc Partnership Program. Infrastructure support from ICMR (Center for Advanced Study in Molecular Medicine), DST (FIST), and UGC-CAS (special assistance) is acknowledged. UC acknowledges the IISc fellowship. The funders had no role in study design, data collection and analysis, decision to publish, or preparation of the manuscript. This work was also supported by the Department of Biotechnology (BT/PR32489/BRB/10/1786/2019), DBT-NBACD (BT/HRD-NBA-NWB/38/2019-20) and Science and Engineering Research Board (CRG/2019/000281) to S.R.G.S. DBT-JRF (DBT/2016/IISc/717) to P.B.

Author Contributions

UC and DC have conceived the study and designed the experiments. UC has performed all the experiments and participated in acquiring the data. UC and PB has analyzed the data, constructed the figures, and wrote the original draft of the manuscript. UC. PB, DC and GSR have participated in the proofreading and editing of the manuscript. DC has supervised the study and helped in fund acquisition. All the authors have read and approved the manuscript.

References:

[1] A. Haraga, M. B. Ohlson, and S. I. Miller, “Salmonellae interplay with host cells,” Jan. 2008. doi: 10.1038/nrmicro1788.

[2] F. W. Brenner, R. G. Villar, F. J. Angulo, R. Tauxe, and B. Swaminathan, “GUEST COMMENTARY Salmonella Nomenclature,” 2000.

[3] D. Pradhan and V. Devi Negi, “Stress-induced adaptations in Salmonella: A ground for shaping its pathogenesis,” Dec. 01, 2019, *Elsevier GmbH*. doi: 10.1016/j.micres.2019.126311.

[4] S. Ferguson *et al.*, “Coordinated Actions of Actin and BAR Proteins Upstream of Dynamin at Endocytic Clathrin-Coated Pits,” *Dev Cell*, vol. 17, no. 6, pp. 811–822, Dec. 2009, doi: 10.1016/j.devcel.2009.11.005.

[5] D. Zhou, L. M. Chen, L. Hernandez, S. B. Shears, and J. E. Galán, “A Salmonella inositol polyphosphatase acts in conjunction with other bacterial effectors to promote host cell actin cytoskeleton rearrangements and bacterial internalization,” *Mol Microbiol*, vol. 39, no. 2, pp. 248–260, 2001, doi: 10.1046/j.1365-2958.2001.02230.x.

[6] C. S. Bakshi, V. P. Singh, M. W. Wood, P. W. Jones, T. S. Wallis, and E. E. Galyov, “Identification of SopE2, a Salmonella Secreted Protein Which Is Highly Homologous to SopE and Involved in Bacterial Invasion of Epithelial Cells,” 2000. [Online]. Available: http://genome.wustl.edu/gsc/bacterial/salmonella.shtml

[7] W.-D. Hardt, L.-M. Chen, K. E. Schuebel, X. R. Bustelo, and J. E. Galá, “S. typhimurium Encodes an Activator of Rho GTPases that Induces Membrane Ruffling and Nuclear Responses in Host Cells,” 1998.

[8] K. C. Boddy *et al.*, “Salmonella effector SopD promotes plasma membrane scission by inhibiting Rab10,” *Nat Commun*, vol. 12, no. 1, Dec. 2021, doi: 10.1038/s41467-021-24983-z.

[9] J.-P. Gorvel and S. Méresse, “Maturation steps of the Salmonella-containing vacuole,” 2001.

[10] D. Drecktrah *et al.*, “Dynamic behavior of salmonella-induced membrane tubules in epithelial cells,” *Traffic*, vol. 9, no. 12, pp. 2117–2129, 2008, doi: 10.1111/j.1600-0854.2008.00830.x.

[11] Fran. Garcia-del Portillo, M. B. Zwick, K. Yin Leung, and B. Brett Finlay, “Salmonella induces the formation of filamentous structures containing lysosomal membrane glycoproteins in epithelial cells,” 1993. [Online]. Available: https://www.pnas.org

[12] J. C. Santos *et al.*, “The COPII complex and lysosomal VAMP7 determine intracellular Salmonella localization and growth,” *Cell Microbiol*, vol. 17, no. 12, pp. 1699–1720, Dec. 2015, doi: 10.1111/cmi.12475.

[13] T. Reuter, S. Vorwerk, V. Liss, T. C. Chao, M. Hensel, and N. Hansmeier, “Proteomic Analysis of Salmonella-modified Membranes Reveals Adaptations to Macrophage Hosts,” *Molecular and Cellular Proteomics*, vol. 19, no. 5, pp. 900–912, May 2020, doi: 10.1074/mcp.RA119.001841.

[14] S. M. Eswarappa, V. D. Negi, S. Chakraborty, B. K. C. Sagar, and D. Chakravortty, “Division of the Salmonella-containing vacuole and depletion of acidic lysosomes in Salmonella-infected host cells are novel strategies of Salmonella enterica to avoid lysosomes,” *Infect Immun*, vol. 78, no. 1, pp. 68–79, Jan. 2010, doi: 10.1128/IAI.00668-09.

[15] N. A. Buchmeiert and F. Heffront, “Inhibition of Macrophage Phagosome-Lysosome Fusion by Salmonella typhimurium,” 1991. [Online]. Available: https://journals.asm.org/journal/iai

[16] “R. Beuzon *et al.*, Salmonella maintains the integrity of its intracellular vacuole through the action of SifA” The EMBO journal, 2000.

[17] D. W. Holden, “Trafficking of the Salmonella vacuole in macrophages,” 2002. doi: 10.1034/j.1600-0854.2002.030301.x.

[18] Friedman *et al*., ER tubules mark site of mitochondrial division, 2011, Science

[19] R. Fernández-Busnadiego, Y. Saheki, and P. De Camilli, “Three-dimensional architecture of extended synaptotagmin-mediated endoplasmic reticulum-plasma membrane contact sites,” *Proc Natl Acad Sci U S A*, vol. 112, no. 16, pp. E2004–E2013, Apr. 2015, doi: 10.1073/pnas.1503191112.

[20] Y. C. Wong, D. Ysselstein, and D. Krainc, “Mitochondria-lysosome contacts regulate mitochondrial fission via RAB7 GTP hydrolysis,” *Nature*, vol. 554, no. 7692, pp. 382–386, Feb. 2018, doi: 10.1038/nature25486.

[21] H.-J. Wang, G. Guay, L. Pogan, R. Sauvé, and I. R. Nabi, “JCB Report Calcium Regulates the Association between Mitochondria and a Smooth Subdomain of the Endoplasmic Reticulum,” 2000. [Online]. Available: http://www.jcb.org

[22] A. A. Rowland, P. J. Chitwood, M. J. Phillips, and G. K. Voeltz, “ER contact sites define the position and timing of endosome fission,” *Cell*, vol. 159, no. 5, pp. 1027–1041, Nov. 2014, doi: 10.1016/j.cell.2014.10.023.

[23] W. K. Ji, R. Chakrabarti, X. Fan, L. Schoenfeld, S. Strack, and H. N. Higgs, “Receptor-mediated Drp1 oligomerization on endoplasmic reticulum,” *Receptor-mediated Drp1 oligomerization on endoplasmic reticulum*, vol. 216, no. 12, p. 190538, 2017, doi: 10.1101/190538.

[24] E. Smirnova, L. Griparic, D.-L. Shurland, and A. M. Van Der Bliek, “Dynamin-related Protein Drp1 Is Required for Mitochondrial Division in Mammalian Cells,” 2001.

536 [25] Rebecca Stanhope et al., IncV, a FFAT motif containing Chlamydia protein, tethers the
537 endoplasmic reticulum to the pathogen containing vacuole, 2017, PNAS

538 [26] G. Boncompain, C. Müller, V. Meas-Yedid, P. Schmitt-Kopplin, P. B. Lazarow, and A. Subtil, "The
539 intracellular bacteria Chlamydia hijack peroxisomes and utilize their enzymatic capacity to
540 produce bacteria-specific phospholipids," *PLoS One*, vol. 9, no. 1, Jan. 2014, doi:
541 10.1371/journal.pone.0086196.

542 [27] J. Sedzicki *et al.*, "3D correlative electron microscopy reveals continuity of Brucellacontaining
543 vacuoles with the endoplasmic reticulum," *J Cell Sci*, vol. 131, no. 4, Feb. 2018, doi:
544 10.1242/jcs.210799.

545 [28] M. Li, I. Tripathi-Giesgen, B. A. Schulman, W. Baumeister, and F. Wilfling, "In situ snapshots along
546 a mammalian selective autophagy pathway," *Proc Natl Acad Sci U S A*, vol. 120, no. 12, Mar. 2023,
547 doi: 10.1073/pnas.2221712120.

548 [29] K. A. Datsenko and B. L. Wanner, "One-step inactivation of chromosomal genes in Escherichia coli
549 K-12 using PCR products," 2000. [Online]. Available: www.pnas.orgcgidoi10.1073pnas.120163297

550 [30] S. Wang, H. Tukachinsky, F. B. Romano, and T. A. Rapoport, "Cooperation of the ER-shaping
551 proteins atlastin, lunapark, and reticulons to generate a tubular membrane network," 2016, doi:
552 10.7554/eLife.18605.001.

553 [31] Y. Shibata *et al.*, "The reticulon and Dp1/Yop1p proteins form immobile oligomers in the tubular
554 endoplasmic reticulum," *Journal of Biological Chemistry*, vol. 283, no. 27, pp. 18892–18904, Jul.
555 2008, doi: 10.1074/jbc.M800986200.

556 [32] N. Zurek, L. Sparks, and G. Voeltz, "Reticulon short hairpin transmembrane domains are used to
557 shape ER tubules," *Traffic*, vol. 12, no. 1, pp. 28–41, Jan. 2011, doi: 10.1111/j.1600-
558 0854.2010.01134.x.

559 [33] V. Singh, C. Erady, and N. Balasubramanian, "Cell-matrix adhesion controls Golgi organization and
560 function through Arf1 activation in anchorage-dependent cells," *J Cell Sci*, vol. 131, no. 16, Aug.
561 2018, doi: 10.1242/jcs.215855.

562 [34] R. Marwaha, S. B. Arya, D. Jagga, H. Kaur, A. Tuli, and M. Sharma, "The Rab7 effector PLE KHM1
563 binds Arl8b to promote cargo traffic to lysosomes," *Journal of Cell Biology*, vol. 216, no. 4, pp.
564 1051–1070, Apr. 2017, doi: 10.1083/jcb.201607085.

565 [35] Y. Adachi *et al.*, "Drp1 Tubulates the ER in a GTPase-Independent Manner," *Mol Cell*, vol. 80, no. 4,
566 pp. 621-632.e6, Nov. 2020, doi: 10.1016/j.molcel.2020.10.013.

567 [36] M. H. Alshareef, E. L. Hartland, and K. McCaffrey, "Effectors targeting the unfolded protein
568 response during intracellular bacterial infection," Apr. 01, 2021, *MDPI AG*. doi:
569 10.3390/microorganisms9040705.

570 [37] M. Cirone, “Er stress, upr activation and the inflammatory response to viral infection,” *Viruses*,
571 vol. 13, no. 5, May 2021, doi: 10.3390/v13050798.

572 [38] K. Yamamoto *et al.*, “Transcriptional Induction of Mammalian ER Quality Control Proteins Is
573 Mediated by Single or Combined Action of ATF6α and XBP1,” *Dev Cell*, vol. 13, no. 3, pp. 365–376,
574 Sep. 2007, doi: 10.1016/j.devcel.2007.07.018.

575 [39] H. Yoshida *et al.*, “ATF6 Activated by Proteolysis Binds in the Presence of NF-Y (CBF) Directly to the
576 cis-Acting Element Responsible for the Mammalian Unfolded Protein Response,” 2000.

577 [40] R. Sriburi, S. Jackowski, K. Mori, and J. W. Brewer, “XBP1: A link between the unfolded protein
578 response, lipid biosynthesis, and biogenesis of the endoplasmic reticulum,” *Journal of Cell*
579 *Biology*, vol. 167, no. 1, pp. 35–41, Oct. 2004, doi: 10.1083/jcb.200406136.

580 [41] H. Wu, P. Carvalho, and G. K. Voeltz, “Here, there, and everywhere: The importance of ER
581 membrane contact sites,” *Science (1979)*, vol. 361, no. 6401, Aug. 2018, doi:
582 10.1126/science.aan5835.

583 [42] J. E. Lee, P. I. Cathey, H. Wu, R. Parker, and G. K. Voeltz, “Endoplasmic reticulum contact sites
584 regulate the dynamics of membraneless organelles,” *Science (1979)*, vol. 367, no. 6477, Jan. 2020,
585 doi: 10.1126/science.aay7108.

586 [43] G. K. Voeltz, W. A. Prinz, Y. Shibata, J. M. Rist, and T. A. Rapoport, “A Class of Membrane Proteins
587 Shaping the Tubular Endoplasmic Reticulum,” *Cell*, vol. 124, no. 3, pp. 573–586, Feb. 2006, doi:
588 10.1016/J.CELL.2005.11.047.

589 [44] M. J. Hoyer *et al.*, “A Novel Class of ER Membrane Proteins Regulates ER-Associated Endosome
590 Fission,” *Cell*, vol. 175, no. 1, pp. 254-265.e14, Sep. 2018, doi: 10.1016/j.cell.2018.08.030.

591 [45] W.-K. Ji, A. L. Hatch, R. A. Merrill, S. Strack, and H. N. Higgs, “Actin filaments target the oligomeric
592 maturation of the dynamin GTPase Drp1 to mitochondrial fission sites”, doi:
593 10.7554/eLife.11553.001.

594 [46] L. Domingues, D. W. Holden, and L. J. Mota, “The Salmonella effector SteA contributes to the
595 control of membrane dynamics of Salmonella-containing vacuoles,” *Infect Immun*, vol. 82, no. 7,
596 pp. 2923–2934, 2014, doi: 10.1128/IAI.01385-13.

597 [47] E. D. R. Case, J. A. Smith, T. A. Ficht, J. E. Samuel, and P. De Figueiredo, “Space: A Final Frontier for
598 Vacuolar Pathogens,” May 01, 2016, *Blackwell Munksgaard*. doi: 10.1111/tra.12382.

599 [48] C. L. Birmingham, A. C. Smith, M. A. Bakowski, T. Yoshimori, and J. H. Brumell, “Autophagy
600 controls Salmonella infection in response to damage to the Salmonella-containing vacuole,”
601 *Journal of Biological Chemistry*, vol. 281, no. 16, pp. 11374–11383, Apr. 2006, doi:
602 10.1074/jbc.M509157200.

603 [49] Tilney *et al*., How the parasitic bacterium Legionella pneumophila modifies its phagosome and
604 transforms it into rough ER implications for conversion of plasma membrane to the ER
605 membrane, 2001, Journal of Cell Science.

606 [50] J. M. Kimmey and C. L. Stallings, "Bacterial Pathogens versus Autophagy: Implications for
607 Therapeutic Interventions," Dec. 01, 2016, *Elsevier Ltd*. doi: 10.1016/j.molmed.2016.10.008.

608 [51] C. Pujol *et al.*, "Yersinia pestis can reside in autophagosomes and avoid xenophagy in murine
609 macrophages by preventing vacuole acidification," *Infect Immun*, vol. 77, no. 6, pp. 2251–2261,
610 Jun. 2009, doi: 10.1128/IAI.00068-09.

611 [52] K. A. Rzomp, L. D. Scholtes, B. J. Briggs, G. R. Whittaker, and M. A. Scidmore, "Rab GTPases are
612 recruited to chlamydial inclusions in both a species-dependent and species-independent
613 manner," *Infect Immun*, vol. 71, no. 10, pp. 5855–5870, Oct. 2003, doi: 10.1128/IAI.71.10.5855-
614 5870.2003.

615 [53] F. S. Mesquita, M. Thomas, M. Sachse, A. J. M. Santos, R. Figueira, and D. W. Holden, "The
616 Salmonella deubiquitinase SseI inhibits selective autophagy of cytosolic aggregates," *PLoS Pathog*,
617 vol. 8, no. 6, Jun. 2012, doi: 10.1371/journal.ppat.1002743.

618 [54] L. Zhou *et al.*, "Salmonella spvC Gene Inhibits Autophagy of Host Cells and Suppresses NLRP3 as
619 Well as NLRC4," *Front Immunol*, vol. 12, Jul. 2021, doi: 10.3389/fimmu.2021.639019.

620 [55] R. J. Bastidas, C. A. Elwell, J. N. Engel, and R. H. Valdivia, "Chlamydial intracellular survival
621 strategies," *Cold Spring Harb Perspect Med*, vol. 3, no. 5, May 2013, doi:
622 10.1101/cshperspect.a010256.

623 [56] K. McGourty, T. L. Thurston, S. A. Matthews, L. Pinaud, L. J. Mota, and D. W. Holden, "Salmonella
624 inhibits retrograde trafficking of mannose-6-phosphate receptors and lysosome function," *Science*
625 *(1979)*, vol. 338, no. 6109, pp. 963–967, Nov. 2012, doi: 10.1126/science.1227037.

626 [57] D. G. McEwan *et al.*, "PLEKHM1 regulates salmonella-containing vacuole biogenesis and
627 infection," *Cell Host Microbe*, vol. 17, no. 1, pp. 58–71, Jan. 2015, doi:
628 10.1016/j.chom.2014.11.011.

629 [58] A. Sindhwani, S. B. Arya, H. Kaur, D. Jagga, A. Tuli, and M. Sharma, "Salmonella exploits the host
630 endolysosomal tethering factor HOPS complex to promote its intravacuolar replication," *PLoS*
631 *Pathog*, vol. 13, no. 10, Oct. 2017, doi: 10.1371/journal.ppat.1006700.

632 [59] J. Bernal-Bayard, E. Cardenal-Muñoz, and F. Ramos-Morales, "The salmonella type III secretion
633 effector, Salmonella Leucine-rich Repeat Protein (SlrP), targets the human chaperone ERdj3,"
634 *Journal of Biological Chemistry*, vol. 285, no. 21, pp. 16360–16368, May 2010, doi:
635 10.1074/jbc.M110.100669.

636 [60] A. N. Antoniou *et al.*, “Salmonella exploits HLA-B27 and host unfolded protein responses to
637 promote intracellular replication,” *Ann Rheum Dis*, vol. 78, no. 1, pp. 74–82, Jan. 2019, doi:
638 10.1136/annrheumdis-2018-213532.

639 [61] J. Kriston-Vizi *et al.*, “Salmonella Exhibit Altered Cellular Localization in the Presence of HLA-B27
640 and Codistribute with Endo-Reticular Membrane,” *J Immunol Res*, vol. 2022, 2022, doi:
641 10.1155/2022/9493019.

642 [62] S. E. McQuate *et al.*, “Long-term live-cell imaging reveals new roles for Salmonella effector
643 proteins SseG and SteA,” *Cell Microbiol*, vol. 19, no. 1, Jan. 2017, doi: 10.1111/cmi.12641.

644 [63] K. Geddes, M. Worley, G. Niemann, and F. Heffron, “Identification of new secreted effectors in
645 Salmonella enterica serovar typhimurium,” *Infect Immun*, vol. 73, no. 10, pp. 6260–6271, Oct.
646 2005, doi: 10.1128/IAI.73.10.6260-6271.2005.

647 [64] L. Domingues *et al.*, “The Salmonella effector SteA binds phosphatidylinositol 4-phosphate for
648 subcellular targeting within host cells,” *Cell Microbiol*, vol. 18, no. 7, pp. 949–969, Jul. 2016, doi:
649 10.1111/cmi.12558.

650 [65] I. Derré, R. Swiss, and H. Agaisse, “The lipid transfer protein CERT interacts with the Chlamydia
651 inclusion protein IncD and participates to ER-Chlamydia inclusion membrane contact sites,” *PLoS*
652 *Pathog*, vol. 7, no. 6, Jun. 2011, doi: 10.1371/journal.ppat.1002092.

653 [66] A. M. Kolodziejek *et al.*, “Salmonella Translocated Effectors Recruit OSBP1 to the Phagosome to
654 Promote Vacuolar Membrane Integrity,” *Cell Rep*, vol. 27, no. 7, pp. 2147-2156.e5, May 2019, doi:
655 10.1016/j.celrep.2019.04.021.

656 [67] K. Liu, L. Kong, D. B. Graham, K. L. Carey, and R. J. Xavier, “SAC1 regulates autophagosomal
657 phosphatidylinositol-4-phosphate for xenophagy-directed bacterial clearance,” *Cell Rep*, vol. 36,
658 no. 4, Jul. 2021, doi: 10.1016/j.celrep.2021.109434.

659 [68] D. Chen *et al.*, “Systematic reconstruction of an effector-gene network reveals determinants of
660 Salmonella cellular and tissue tropism,” *Cell Host Microbe*, vol. 29, no. 10, pp. 1531-1544.e9, Oct.
661 2021, doi: 10.1016/j.chom.2021.08.012.

662 [69] V. Göser, A. Kehl, J. Röder, and M. Hensel, “Role of the ESCRT-III complex in controlling integrity of
663 the Salmonella-containing vacuole,” *Cell Microbiol*, vol. 22, no. 6, Jun. 2020, doi:
664 10.1111/cmi.13176.

665

666

667

668

669

670

671

672

673 **Legends to the Figures**

674 **Fig:1-*Salmonella* infection leads to the activation of UPR and expansion of the**

675 **Endoplasmic Reticulum**

676 (A) Representative confocal microscopic images of uninfected and infected HeLa cells
677 with STM WT mCh or STM*ΔssaV* mCh at MOI 10, 16h post-infection and immuno-
678 stained against ATF4, LAMP1 and DAPI. (B) Represents the quantification of Cell Total
679 Corrected Fluorescence (CTCF) intensity of ATF4 inside the nucleus, data is
680 representative of n=100-120 cells, from 4 independent experiments, mean±SD (C)
681 Representative confocal microscopic images of uninfected and infected HeLa cells with
682 STM WT mCh or STM*ΔssaV* mCh at MOI 10, 16h post infection and immuno-stained
683 against ATF6, LAMP1 and DAPI. (D) Represents the quantification of Cell Total
684 Corrected Fluorescence (CTCF) intensity of ATF6 inside the nucleus, data is
685 representative of n=60-90 cells from 3 independent experiments, mean±SD (E)
686 Representative confocal microscopic images of uninfected and infected HeLa cells with
687 STM WT mCh or STM*ΔssaV* mCh at MOI 10, 16-hour post-infection and immuno-
688 stained against XBP1, LAMP1, and DAPI (F) Represents the quantification of Cell Total

689 Corrected Fluorescence (CTCF) intensity of XBP1 inside the nucleus, data is
690 representative of n=60-90 cells from 3 independent experiments, mean±SD (G)
691 Quantitative real-time PCR of *Rtn4a* (H) and *Climp63*, N=3, n=3, mean±SEM (I)
692 Confocal microscopic images of Un-infected and infected HeLa cell showing ER
693 expansion (J) Represents the quantification of tubular ER, data is representative of n=100-
694 150 cells from 4 independent experiments, mean±SD. Student's t-test was used to analyze
695 the data ****<0.0001, ***<0.001, **<0.01, *<0.05.

696 **Fig-2: Expansion of ER tubules facilitates SCV proliferation and its division**

697 (A) Represents the ICSA upon overexpression of Rtn4a, data is representative of N=3,
698 n=3 mean± SEM (B) ICSA upon Rtn4a knockdown in HeLa cells, data is representative of
699 N=3, n=3 mean± SEM (C) Representative confocal microscopy images of SCV number
700 per cell upon overexpression of mCh-EV, sec61β-mCh, and mCh-Climp63, 16h post
701 infection (D) Quantification of the number of SCV per cell, 16h post infection, data is
702 representative of n=40-60 cells from 2 independent experiments (E) Snapshot of live cell
703 imaging of *Salmonella* infected HeLa cells, White arrowhead represent the ER overlap at
704 dividing bacteria. White line along the length of bacteria represent the portion used for
705 line scan. (F) Showing the line scan of images. Blue arrows represent the snapshot for
706 which the line scan is analyzed (snapshots 3 and 4) (G) Quantification of SCV fission
707 events marked by ER, data is representative of n=11 SCV fission events from 4
708 independent experiments (H) Confocal microscopic images representing SCV fission
709 events marked by ER, at center or adjacent (I) Quantification of fission events in fixed
710 images marked by ER, data is representative of n=49 SCV fission events from 4

711 independent experiments. White arrowhead represent the ER overlap at dividing SCV.
712 Student's t-test was used to analyze the data ****<0.0001, ***<0.001, **<0.01, *<0.05.

713 **Fig-3: *Salmonella* translocated effector SteA is crucial for maintaining SCV contacts**
714 **with ER, resulting in a single bacterium per vacuole**

715 (A) Represents confocal microscopy images showing SCV formed by STM WT and
716 STM*ΔsteA,* 16h post-infection (B) Quantification of the number of cells showing multiple
717 bacteria in one vacuole, 16h post-infection, data is representative of n=120-150 cells from
718 3 independent experiments, mean±SEM (C) Representative confocal image of infected
719 HeLa cell showing contact between SteA-HA and ER, arrowheads represent interaction
720 between ER and SteA-HA (D) Confocal images represents the colocalization of ER with
721 SCV formed by either STM WT or STM*ΔsteA,* 16h post-infection (E) Quantification of
722 colocalization coefficient of ER marker RFP KDEL with SCV marker LAMP1, Data is
723 representative of n=80-100 cells from 2 independent experiments, 16h post infection,
724 mean±SD. Student's t test was used to analyse the data ****<0.0001, ***<0.001,
725 **<0.01, *<0.05.

726 **Fig-4: STM*ΔsteA* shows a defect in proliferation and pathogenicity *in vivo***

727 (A) Intracellular survival assay of STM WT, STM*ΔsteA*, and STM*ΔsteA:steA* in HeLa
728 cells, data is representative of N=3,n=3, mean±SEM. (B) Line representation to quantify
729 SCV diameter where red line indicates the length of SCV used for quantification (C)
730 Quantification of SCV diameter, data is representative of 100-150 cells from 3
731 independent experiments, 16h post-infection, mean±SD (D) Representative microscopy
732 images showing colocalization of LC3B with SCV, 16h post-infection(E) Quantification

733 of colocalization coefficient of LC3B with SCV, data is representative of n=100-130 cells
734 from 3 independent experiments, mean±SD (F) outline of experimental procedure of mice
735 infection through intraperitoneal route (G) CFU enumeration in Spleen and (H) liver, data
736 is representative of N=2, n=5 mice per cohort (I) Outline of experimental procedure of
737 mice infection through oral gavage and dissected on day 5 post infection (J) CFU
738 enumeration in organs like Spleen (K) Liver (L) and MLN, data is representative of N=3,
739 n=5 mice per cohort, mean±SD (M) Survival curve of cohort of mice infected with STM
740 WT and STM*ΔsteA,* n=8 mice per cohort. Mann-Whitney test was performed to obtain
741 statistical significance for *in vivo* data. Student's t-test was used to analyze the data from
742 fig 4A-4E. ****<0.0001, ***<0.001, **<0.01, *<0.05.

743

744

745

746

747

Graphical Abstract

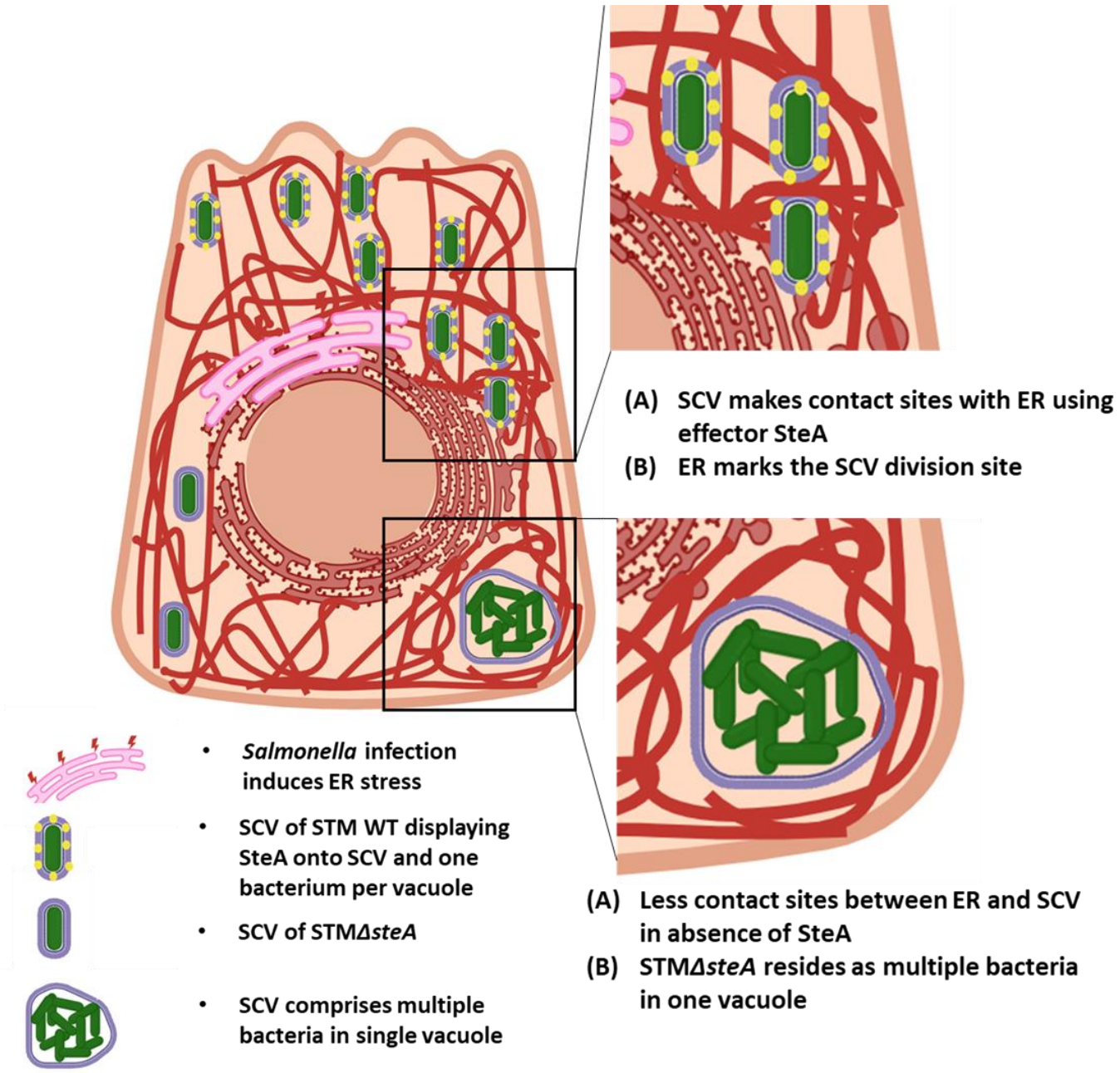

Fig:1 *Salmonella* infection leads to the activation of UPR and expansion of the Endoplasmic Reticulum

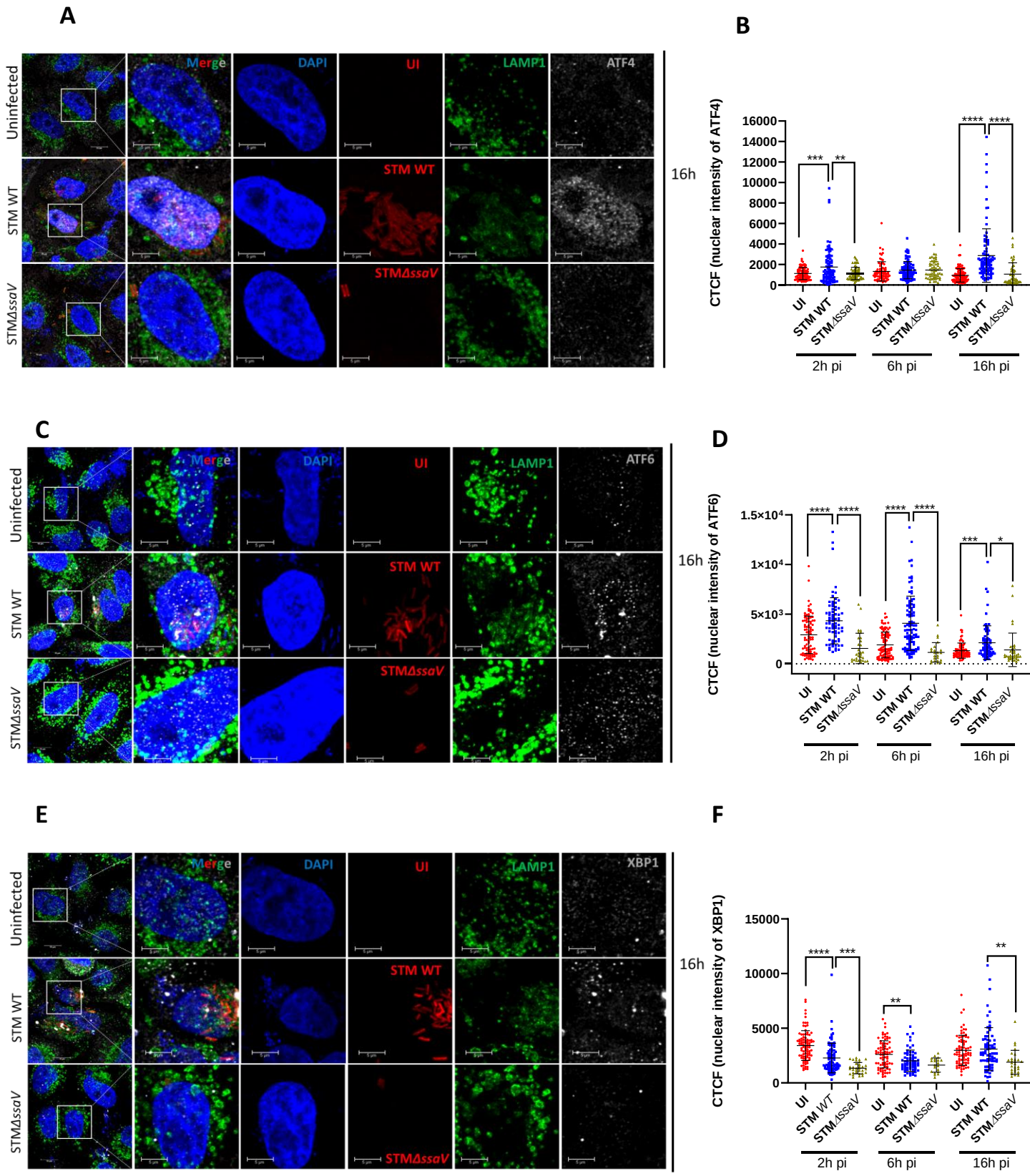

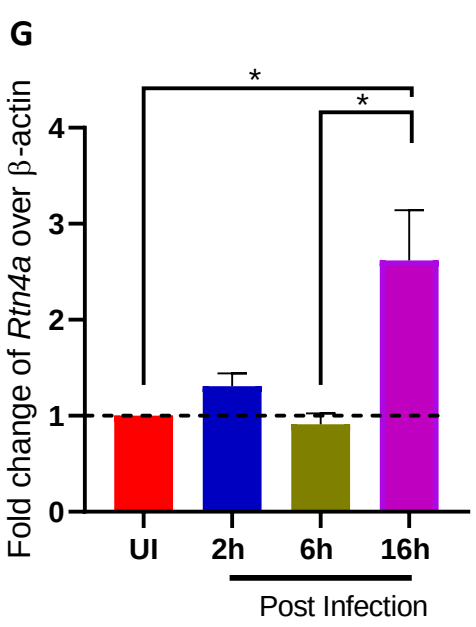
G
Fold change of Rtn4a over β-actin
*
*
4
3
2
1
0
UI
2h
6h
16h
Post Infection

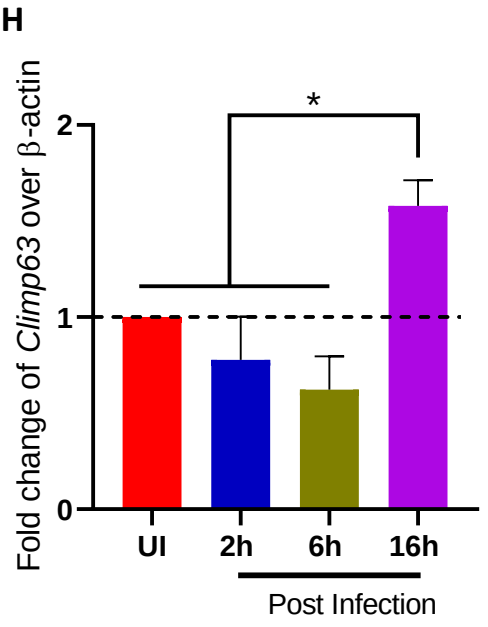
H
Fold change of Climp63 over β-actin
*
2
1
0
UI
2h
6h
16h
Post Infection

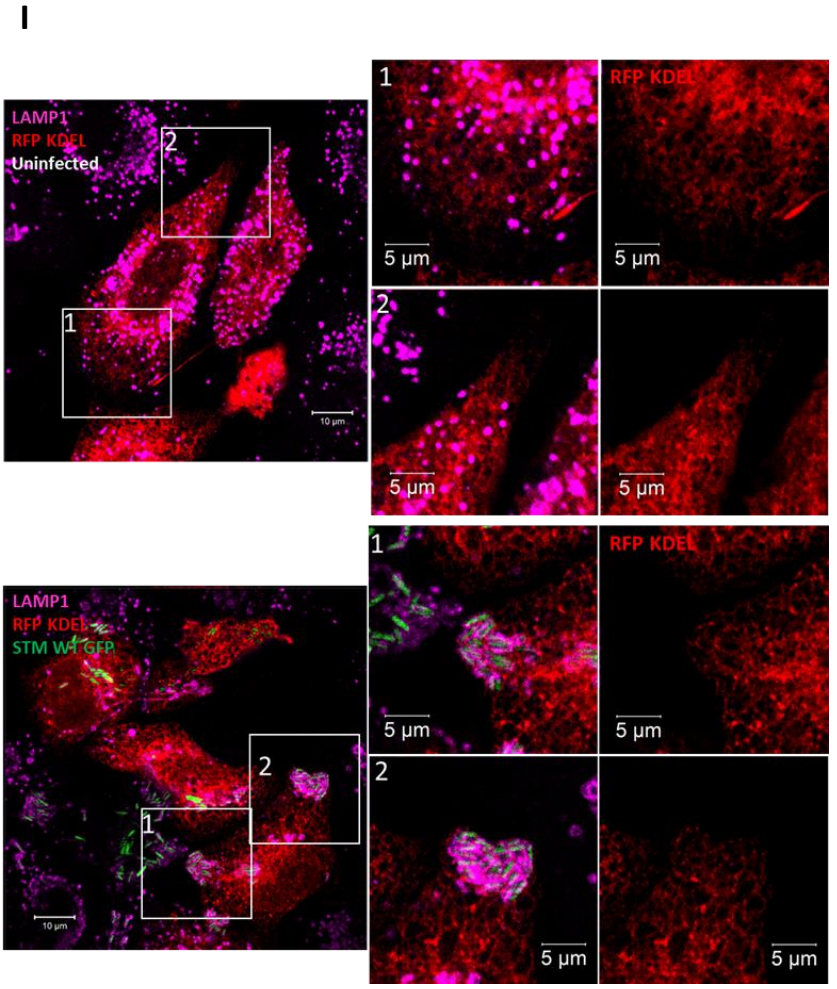
I
LAMP1
RFP KDEL
Uninfected
1
2
10 µm
RFP KDEL
5 µm
LAMP1
RFP KDEL
STM WT GFP

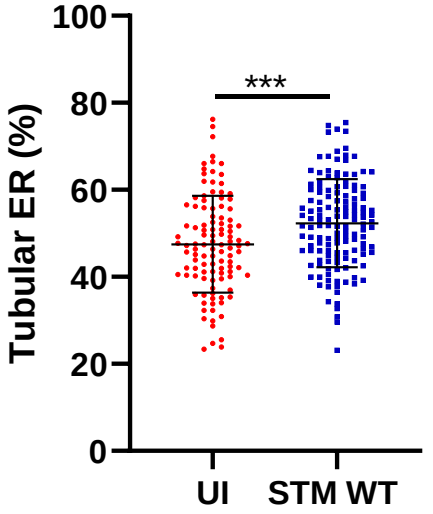
J
Tubular ER (%)
***
100
80
60
40
20
0
UI
STM WT

Fig 2: Expansion of ER tubules facilitates SCV proliferation and its division

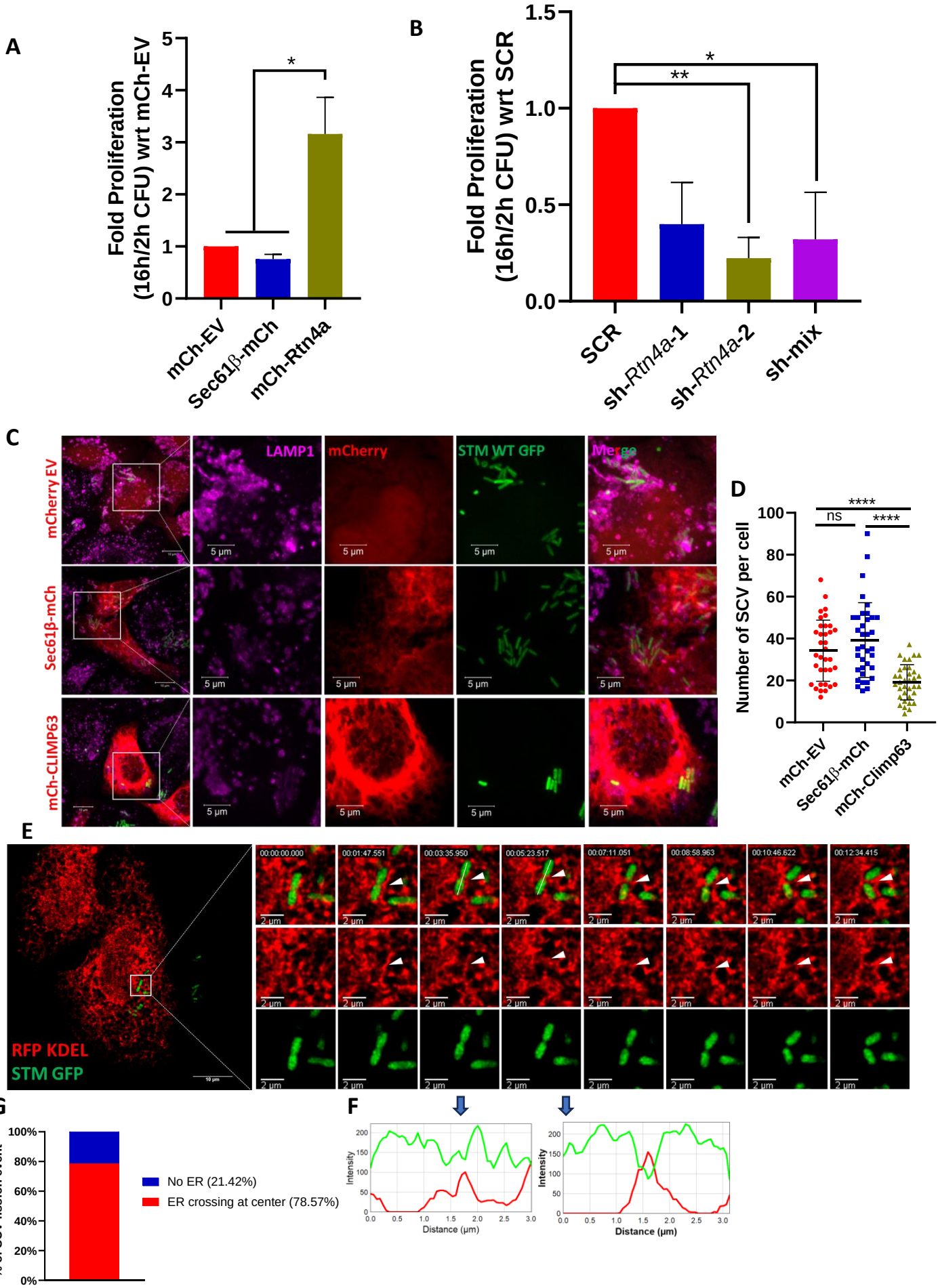

H

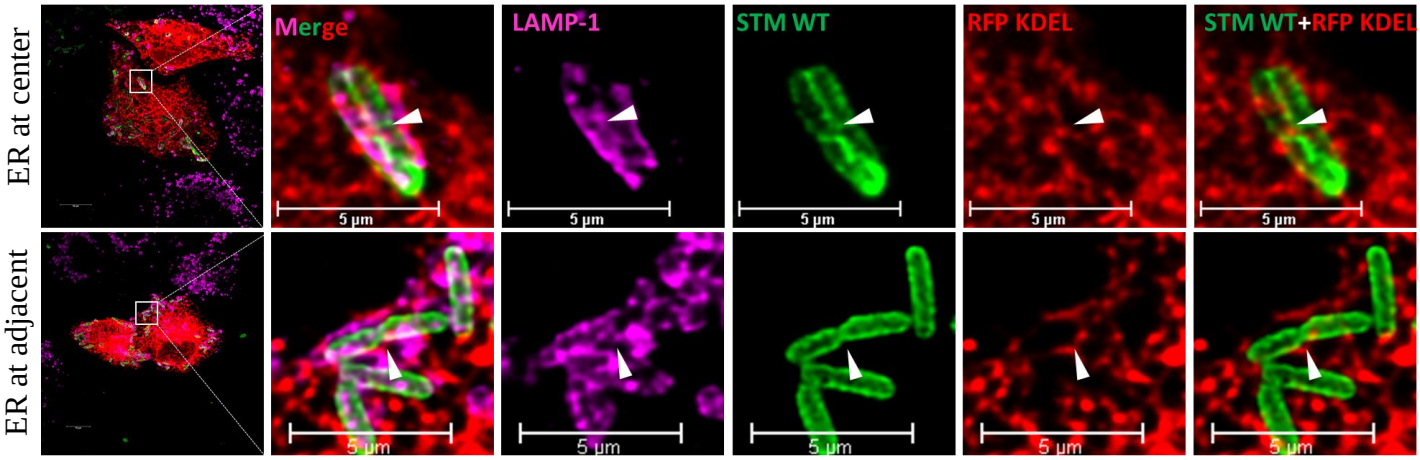
ER at center
ER at adjacent
Merge
LAMP-1
STM WT
RFP KDEL
STM WT+RFP KDEL
5 µm

I

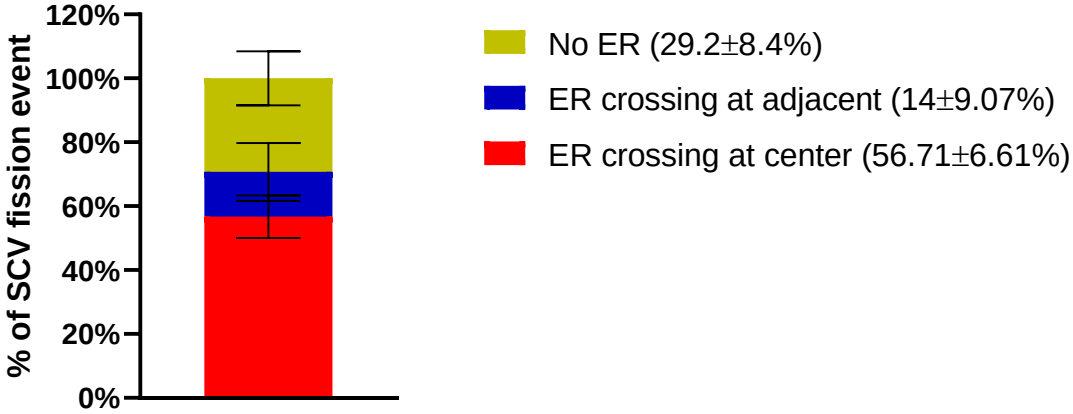
% of SCV fission event
120%
100%
80%
60%
40%
20%
0%
No ER (29.2±8.4%)
ER crossing at adjacent (14±9.07%)
ER crossing at center (56.71±6.61%)

Fig 3: *Salmonella* translocated effector steA is crucial for maintaining SCV contacts with ER resulting in a single bacterium per vacuole state

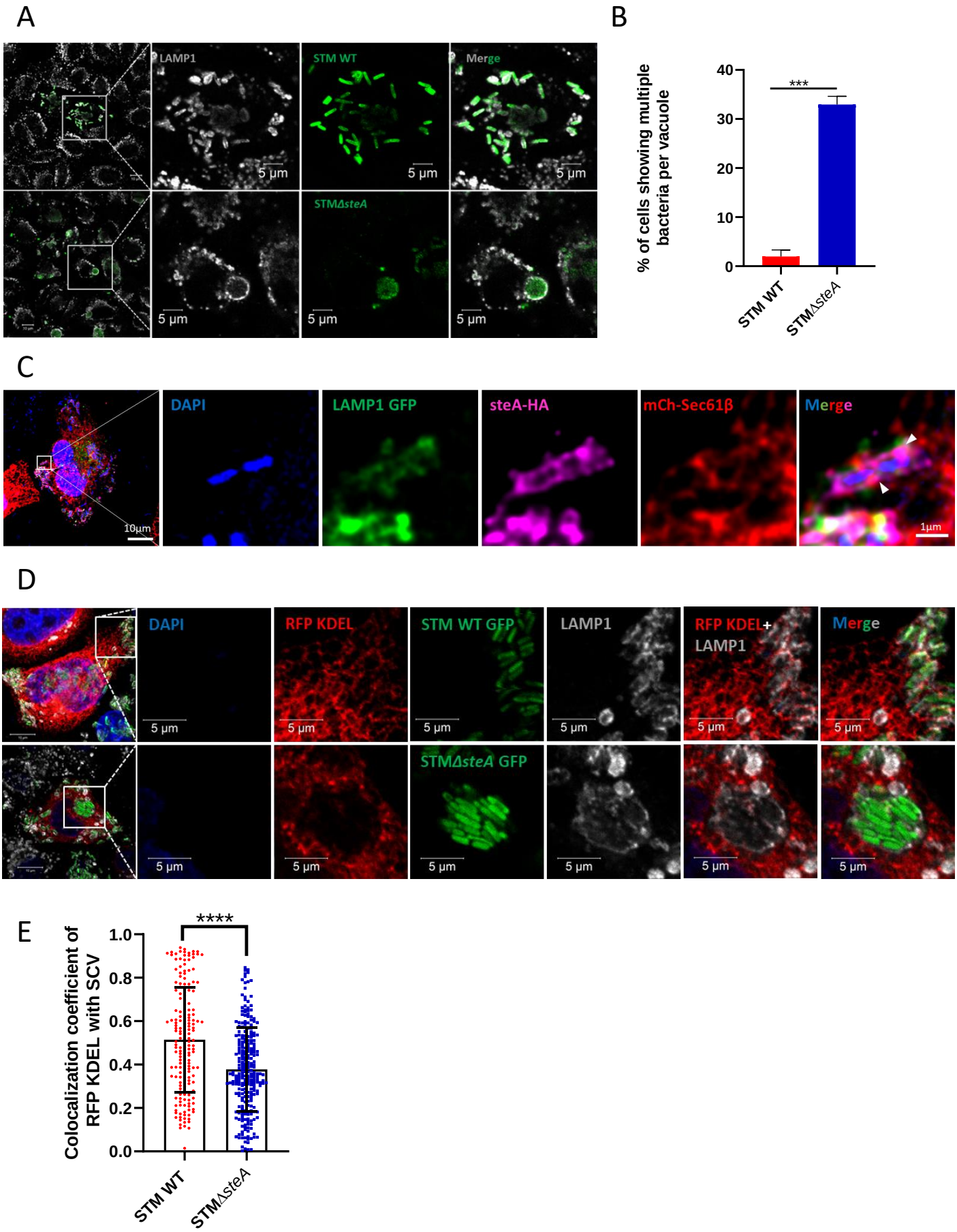

Fig 4: STM*ΔsteA* shows a defect in proliferation and pathogenicity *in vivo*

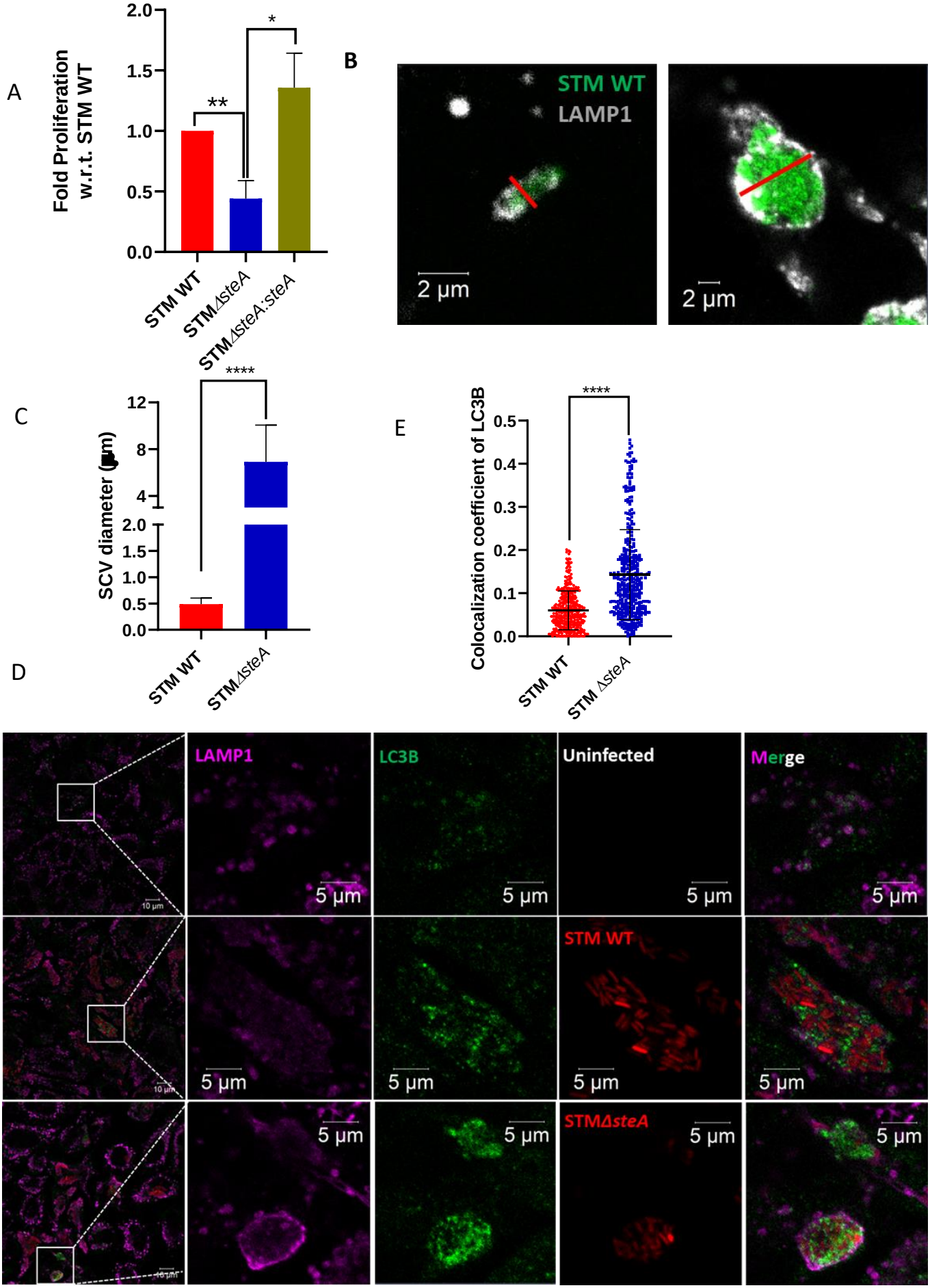

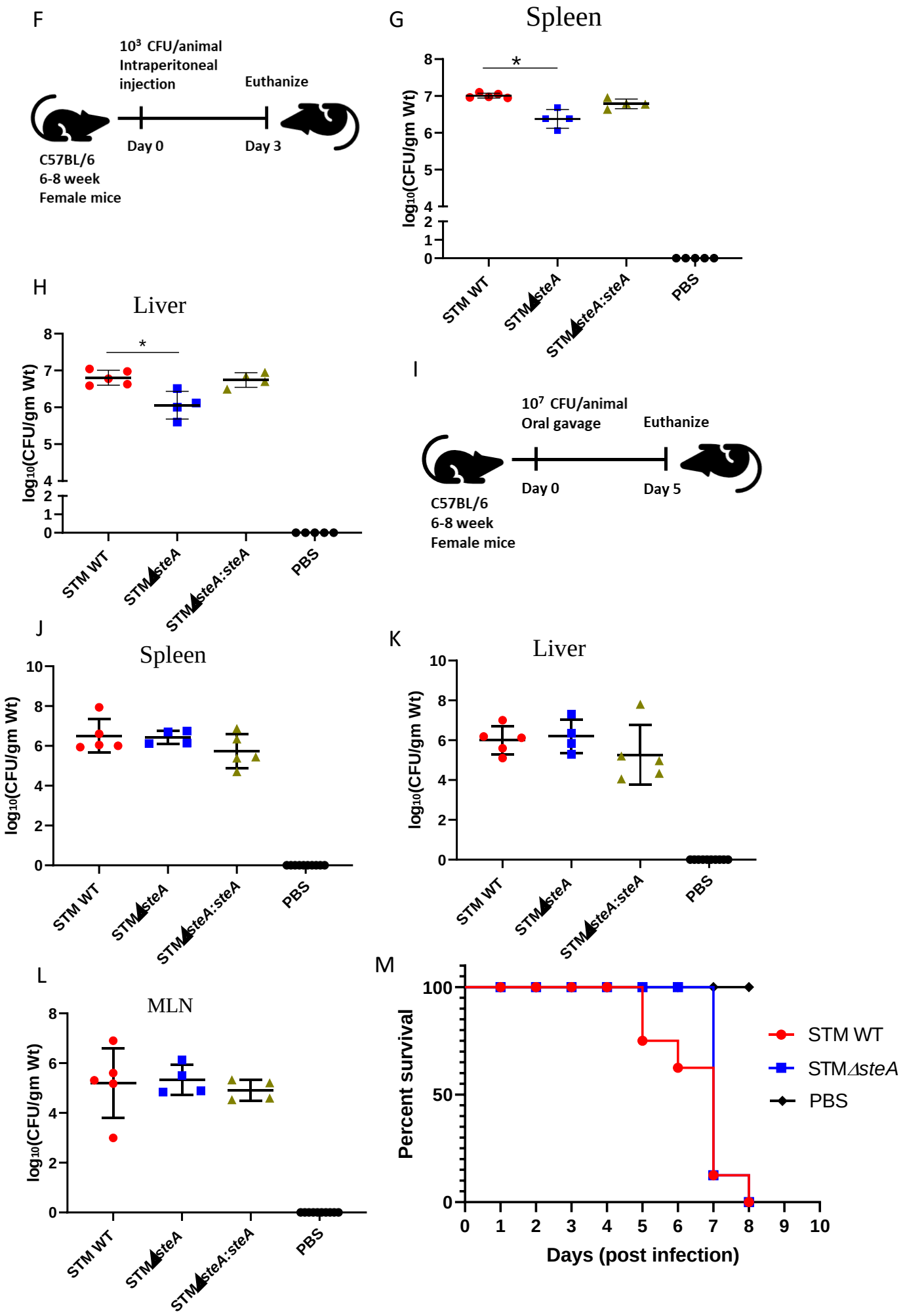
F
10³ CFU/animal
Intraperitoneal
injection
Euthanize
Day 0
Day 3
C57BL/6
6-8 week
Female mice
G
Spleen
log10(CFU/gm Wt)
STM WT
STMΔsteA
STMΔsteA:steA
PBS
H
Liver
I
10⁷ CFU/animal
Oral gavage
Euthanize
Day 0
Day 5
C57BL/6
6-8 week
Female mice
J
Spleen
K
Liver
L
MLN
M
Percent survival
Days (post infection)
STM WT
STMΔsteA
PBS